22 K superconductivity in $BaFe_2As_2$ exposed to F_2

G. N. Tam,[1] Hiraku Maruyama,[2] Juan C. Nino,[2] and G. R. Stewart[1]
[1]*Department of Physics, University of Florida, Gainesville, Florida 32611, USA*
[2]*Department of Materials Science and Engineering, University of Florida, Gainesville, Florida 32611, USA*

(Received 24 May 2019; revised 15 July 2020; accepted 6 October 2020; published 20 October 2020)

Several previous reports on undoped $AEFe_2As_2$ (AE = alkaline earth metal) point to drops in resistivity indicative of possible superconductivity and some degree of Meissner effect in the magnetic susceptibility. Also, based on both resistivity and magnetic susceptibility measurements, controlled exposure to water vapor has been shown to induce superconductivity in $AEFe_2As_2$. In our study, $BaFe_2As_2$ single crystals grown using the self-flux method showed a full resistive drop around 22 K and magnetic shielding, when exposed to fluorine gas postgrowth. Our measurements indicate electron (donor) doping via atomic substitution of F for As is concurrent with the observed superconductivity, which sheds light on the likely effect of exposure to water vapor in previous work. Like doping experiments (such as substitution of Co for Fe, P for As, or K for Ba) in $AEFe_2As_2$ to date, the present work is consistent with suppression of the spin density wave transition coincident with the appearance of T_c. In addition to answering the puzzle of superconductivity in undoped or water vapor exposed $AEFe_2As_2$, our results also represent a fast (20 min exposure to 5% F in He) and reliable method suitable for inducing superconductivity in thin films of $AEFe_2As_2$. Some supportive work on $BaFe_2As_2$ exposed to Cl_2 is also presented.

DOI: 10.1103/PhysRevB.102.134507

I. INTRODUCTION

Iron-based superconductors (IBS) are a class of high temperature superconductors discovered in 2006 [1], with T_c = 6 K in LaFePO. The prototypical iron-based superconductor appeared in the form of $LaFeAs(O_{1-x}F_x)$, T_c = 26 K, as reported by Kamihara *et al.* in 2008 [2]. The iron-based superconducting compounds can mostly be separated into four main structural groups: 1111 (LaFeAsO), 111 (LiFeAs), 122 ($BaFe_2As_2$), and 11 (FeSe) [3]. The overall crystal structure of the compounds is typically tetragonal or orthorhombic, but in general it can be described by an insulating layer (e.g., Ba or LaO) nested between conducting iron pnictide or iron chalcogenide layers [4]. Superconductivity via doping in the iron-based superconductors is quite robust, as compared to cuprates, in that it can be achieved via donor doping (e.g., substitution of Co for Fe), acceptor doping (e.g., substitution of K for Ba), or isovalent doping (substitution of P for As) [5]. The original discovery [2] of 26 K superconductivity in the 1111 structure was via substitution of F for O (i.e., donor doping) which facilitates the charge transport in the conducting layer. While the microscopic mechanism responsible for the superconducting pairing is still under debate [3], it is at least theorized to be due to exchange of spin fluctuations [6,7].

In order to attain additional insight into this physical phenomenon, in the present work we focus on $AEFe_2As_2$ (AE = alkaline earth metal) IBS compounds, also known as 122 IBS. In their undoped form, 122 IBS are generally not superconducting under normal conditions, although it is well known that superconductivity can be achieved by applying pressure [8–10] or doping [5,11]. In a few (~4% in our laboratory) cases, nominally undoped, as-grown $BaFe_2As_2$ can exhibit traces of superconductivity with a T_c around 20 K. Such outlier results have long been seen, see, e.g., the work [12] by Tanatar *et al.* who reported two (out of five) samples of undoped $BaFe_2As_2$, which showed significant (up to 25%) drops in resistivity at 20 K. There has been a long discussion about this and similar results, including work by Saha *et al.* [13], who attributed strain to the cause of superconductivity in their undoped $SrFe_2As_2$, and by Kim *et al.* [14], who ruled out strain in their In-flux grown $BaFe_2As_2$. Adding to the puzzle, Hiramatsu *et al.* observed water-vapor-induced superconductivity also around 20 K in $SrFe_2As_2$ thin films [15], opening the possibility that the trace superconductivity observed in some 122's could be due to exposure to air. Hiramatsu *et al.* offer a multitude of possible explanations such as intercalation of oxygen atoms in the *I*9 (4*e*) interstitial site and a reaction between $SrFe_2As_2$ and H_2O, but eventually concluded that the observed shrinking of the *c* axis corresponded to chemical pressure-induced superconductivity.

Typically, doping in $BaFe_2As_2$ results in the separation of the overlapping-in-temperature structural and magnetic transitions, which for undoped $BaFe_2As_2$ both occur at about 138 K [16]. As the doping level is increased and the composition deviates further from the parent compound, the magnetic transition is increasingly suppressed (faster than the structural transition), eventually leading to the emergence of superconductivity and the formation of a superconducting dome [4].

Here we show that by exposing $BaFe_2As_2$ to (the very reactive) fluorine gas, we are able to produce a superconducting layer ~5–10 μm thick on the surface of the nonsuperconducting crystal. The observed effect of the doping process is rather

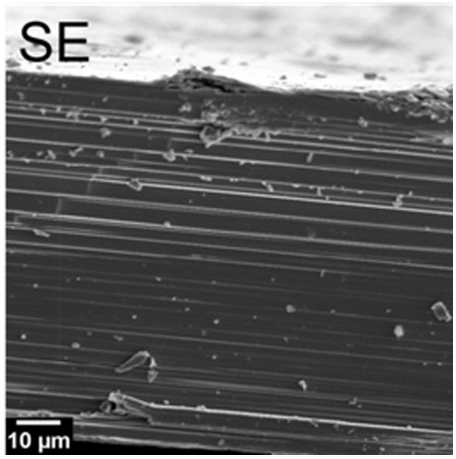

FIG. 1. Scanning electron microscopy image (secondary electron detector, scale shown in lower left corner) of the edge of an undoped flux grown single crystal of $BaFe_2As_2$ prepared as described in the text. Notice the layered stacking apparent in the growth morphology.

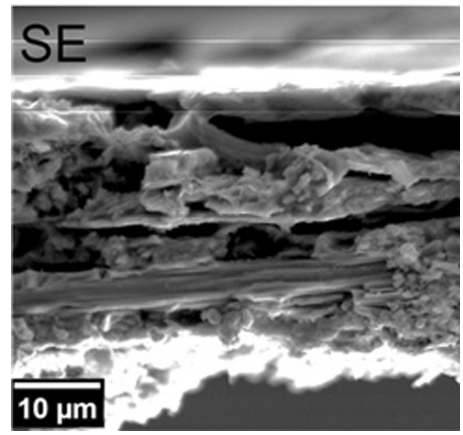

FIG. 2. Scanning electron microscopy image (secondary electron detector, scale shown in lower left corner; note that this is a mechanically polished, thinner ($\sim$40 μm) crystal than shown in Fig. 1) of the edge of a F-doped (20 min exposure) flux grown single crystal of $BaFe_2As_2$ as described in the text. Notice the evident crystal surface degradation due to the F exposure. This sample was characterized by EPMA measurements as discussed later in the text.

unusual for several reasons but primarily because the dopant, due to the reactivity of F, is easily introduced postgrowth and does not result in bulk superconductivity. By systematically characterizing the superconductivity in 122 $BaFe_2As_2$ induced by exposure to F, we further investigate the issue of the cause of the superconductivity observed by Hiramatsu *et al.*, as well as to shed light on the occasional observation of 20 K superconductivity in some nominally undoped 122 IBS. (Partial results on $BaFe_2As_2$ exposed to the less reactive gas Cl are included for completeness at the end of this article.)

II. EXPERIMENTAL

Single-crystalline $BaFe_2As_2$ was grown using the self-flux method [17–19]. Barium (99.9%), iron (99.998%), and arsenic (99.999%) from Alfa Aesar were mixed 1:5:5 in an alumina crucible in an inert atmosphere glove box. The crucible is then sealed in a niobium container with half an atmosphere of high purity argon. The container was heated to 600 °C, where it remained for 24 h, then heated to 1200 °C and soaked for an additional 8 h, followed by a slow cool at 3 °C/h back down to 600 °C. This procedure results in crystals of approximate dimensions of 3 mm × 2 mm × 0.25 mm, which are easily separated mechanically from the FeAs flux. Figure 1 shows a scanning electron microscope image of the edge of such a crystal, emphasizing the layered nature of the crystal growth morphology.

The fluorine treatment was carried out at room temperature in a sealed vessel with 5% fluorine in 95% helium at a pressure of ½ atmosphere. Exposure times typically varied from 20–40 min, with 20 min usually giving a full resistive transition. Shorter exposure times occasionally resulted in incomplete transitions (i.e., resistance does not fully go to zero), discussed further below. Exposure times exceeding 60 min (i.e., three times the usual exposure time necessary for a complete transition) severely compromised the integrity of the crystals and frequently resulted in the crystals crumbling due to the aggressive nature of the fluorine. Even at 20 min of exposure time to F, when viewed from the edge (see Fig. 2), substantial exfoliation of the crystal takes place.

Electron transport measurements were performed using the four-wire configuration. The current was supplied by a Keithley 6220 precision current source. The voltage was measured with a Keithley 2182a nanovoltmeter operating in δ mode to account for thermal heating within the sample. Platinum leads, 0.002" in diameter, were attached with Epotek H20E LV silver epoxy to the as-prepared crystal. The epoxy was cured at 150 °C for 15 min. Because fluorine reacts heavily with the silver epoxy, leads often required reattachment after fluorination. We observed no indication that the silver epoxy, other than the necessity of heating for its curing, affected any properties.

X-ray photoelectron spectroscopy (XPS) was performed using a PHI 5000 VersaProbe II Scanning XPS Microprobe by ULVAC-PHI Inc. Monochromatic x-rays from aluminum were used to irradiate the sample surface. The power was set to 50.0 W with a pass energy of 93.90 eV on a 200-μm diameter spot size. Multiple take-off angles were used to examine the atomic composition with depth. Elemental distribution analysis was performed using Electron Probe Microanalyzer (EPMA, CAMECA, SXFiveFE). Voltage and current were 15 kV and 21 nA, respectively.

III. RESULTS AND DISCUSSION

A. Resistivity

Figure 3 shows the resistivity of a sample prior to and after 20 min of fluorination. At 139.5 K in the fluorinated sample, the drop in resistivity corresponding to both T_S and T_{SDW} is observed. We will argue below that this is due to the undoped portion of the sample (parallel resistance path) and that the F-doped portion of the sample, just as in doping studies on the Ba, Fe, and As sites [20], shows no T_S/T_{SDW} transition. More interestingly, a drop in the resistivity is observed at

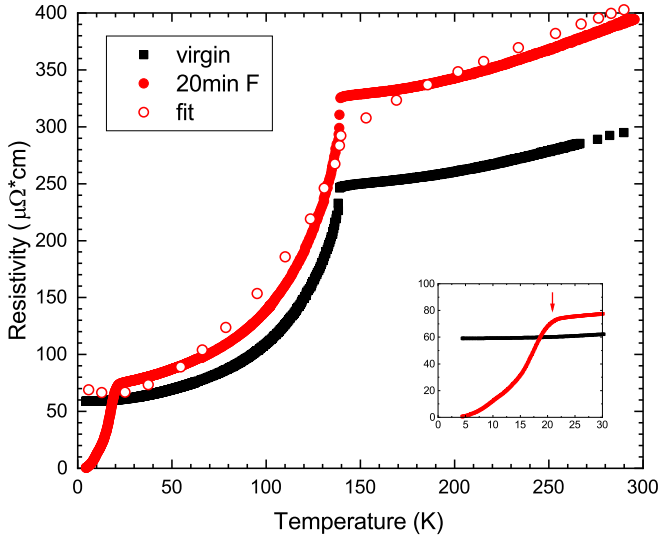

FIG. 3. Resistivity vs temperature of a 25-μm thinned $BaFe_2As_2$ crystal, glued on the bottom and exposed on the top to 20 min of fluorine gas environment showing the appearance of a superconducting transition and an increase in normal state resistivity, presumably due to increased scattering from the fluorine dopant incorporation just as seen [20] with doping with K (for Ba), Co (for Fe) and P (for As). The sample was thinned so that the F penetrates a larger fraction of the sample, giving measurement results more characteristic of F-doped material. The fit corresponding to the open red circles is explained later in the text. The transition is shown on an expanded scale in the inset, with the arrow marking $T_c^{\text{onset}} = 21.6$ K.

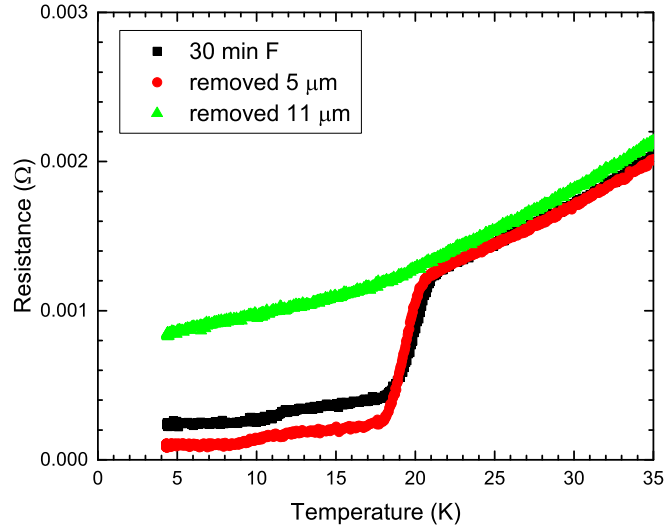

FIG. 4. Depth of the fluorine penetration as determined from resistance vs temperature data on polished samples. A longer reaction time was used to compensate for only one surface being exposed to the fluorine. Only the data above in Fig. 3 were measured taking into account the geometrical conversion factor between resistance and resistivity. Thus, the data shown here and those in succeeding figures are plotted as resistance.

21.6 K in the fluorinated sample in Fig. 3, marking the onset of a superconducting transition. The introduction of fluorine produces scattering sites in the structure, thereby raising the normal state resistivity of the sample. Because of the finite depth penetration of the fluorine, the measured increase in the resistivity depends on the thickness of the crystal. Thicker crystals show less of an increase because the unfluorinated portion of the crystal serves as a shunt, thus more dominating the transport in the normal state. The postgrowth reaction of $BaFe_2As_2$ crystals with fluorine resulted in large variability in the quality of the superconducting resistive transitions (i.e., width of transitions and lowest resistivities reached) but a few characteristics almost always remained consistent: T_c onset always occurred around 22 K $\pm$ 2 K and the T_S/T_{SDW} anomaly in the resistivity contribution from the undoped portion of the sample remained constant to ~5 K.

Because the thickness is an important factor in the interpretation of our resistivity data, before we come to the fit in Fig. 3 we discuss our determination of the thickness of the fluorinated (superconducting) layer and how it compares to the thickness of the sample. The depth of the fluorine penetration was measured on successive polishing of the crystal with a digital comparator with 1-μm resolution. The $BaFe_2As_2$ crystal was glued down flat and polished using 2000 grit polishing paper with a weighted lapping tool to press the sample down onto the polishing paper to minimize tilting/uneven thickness. Removal of 5-μm from the reacted surface shows a very slight decrease in the magnitude of T_c onset as shown in Fig. 4. Necessarily, the electrical contacts were removed and reattached each time the surface was polished. The improved quality of the transition (sharpness of transition and lower achieved resistance) after removing 5 μm shown in Fig. 4 is likely a consequence of the sample being unavoidably annealed [14,21–23] when leads are reattached and the epoxy is cured. Figure 5 below shows an example of the effects of annealing.

As seen in Fig. 4, after removing 11 μm, all traces of superconductivity vanish. Another sample that we applied

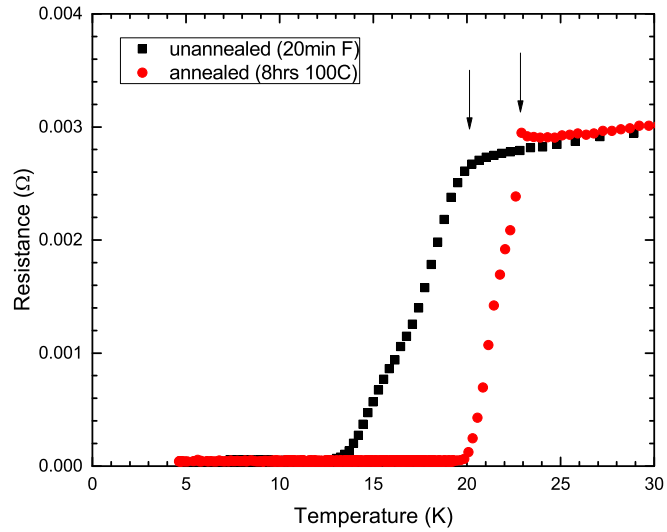

FIG. 5. Resistance vs temperature on a fluorinated sample before (black squares) and after (red circles) 8 h of annealing at 100 °C in air. Arrows indicate T_c^{onset} (approximately 20 and 23 K, respectively). The cause of the small upturn just above T_c in the annealed sample remains a puzzle.

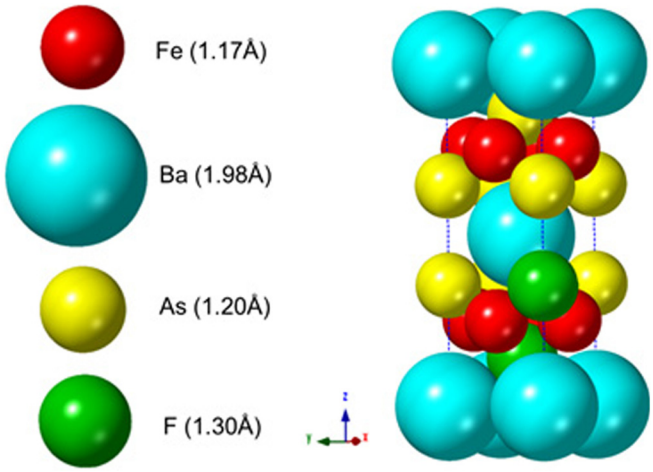

FIG. 6. Crystal structure of F-doped $BaFe_2As_2$ (*I*4*mmm*) indicating the possible 4*e* crystallographic sites for F atoms substituting As atoms. Covalent radius values are indicated in parentheses.

these same methods to also had a clear transition with 5 μm removed and no transition with 10 μm removed. We therefore conclude the maximum fluorine penetration depth is between 5 and 10 μm. Our limitations in accuracy are a result of inhomogeneity in thickness of the crystals, tilting that occurred while gluing down the sample, during the drying of the glue, and during polishing.

Now that we have an estimate of the thickness of the fluorinated layer, we can model the resistance of the 25 μm sample's resistivity shown above in Fig. 3 as being due to 40% (=10/25) of a fluorinated layer (with presumably, as seen [20] in other dopings in the 122 iron-based superconductors after superconductivity is induced, no T_S/T_{SDW} transition) and 60% of the pure, undoped $BaFe_2As_2$ resistivity (black squares in Fig. 3). The fit (open red circles) shown in Fig. 3 used a normal state resistivity for the F-doped fraction of the sample of 1.8 times the resistivity data for $Ba_{0.77}K_{0.23}Fe_2As_2$ as given in Ref. [20]. (The resistivities of Co-doped or P-doped $BaFe_2As_2$ work just as well, with differing multiplicative factors to match the measured F-doped sample data.) The fit shown in Fig. 3, using the normal state resistivity of K-doped $BaFe_2As_2$ times 1.8 (an adjustable parameter) to approximate the resistivity of F-doped $BaFe_2As_2$, is not a bad approximation of the fluorinated sample data over the whole temperature range from T_c to room temperature.

To try to understand the crystallochemical effect of doping F atoms on $BaFe_2As_2$, it is important to recall that the parent crystal structure is body-centered-tetragonal (BCT) at room temperature, transforming to face-centered-orthorhombic below T_S. In the BCT structure, Ba atoms sit on the 2*a* sites, Fe on the 4*d* sites, and As on the 4*e* sites. On the basis of size, charge, and electronegativity considerations, it is clear that fluorine is most likely to either replace arsenic or occupy an interstitial site. Figure 6 shows the unit cell for $BaFe_2As_2$ with fluorine substitution for arsenic. Since the bonding in $BaFe_2As_2$ is expected to be a mix between covalent and ionic, the Shannon's ionic radii [24] were employed for all elements.

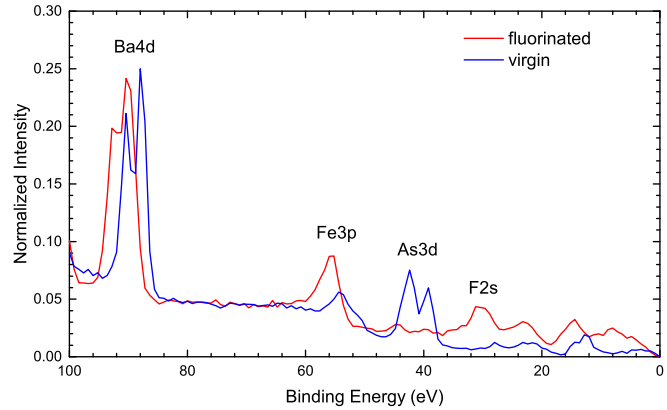

FIG. 7. X-ray photoelectron spectroscopy spectra on untreated (blue) and fluorinated (red) crystals taken at a 90° take-off angle.

B. Characterization of the distribution and effect of the F atoms in $BaFe_2As_2$

The photoelectron spectra for a 90° take-off angle are shown in Fig. 7. In the virgin spectrum, prominent As3*d* peaks can be seen. After 20 min of fluorination, the same twin peaks barely rise above the background, with the additional added feature of the appearance of a F2*s* peak. The shift in the spectrum, most notably in the Ba4*d* peaks, is a result of the change in the binding environment caused by fluorine. The spectra for the other take-off angles measured (30° and 45°) do not reveal any variation with angle for the depth sampled. The suppression of the As3*d* peaks coinciding with the rise of the F2*s* peak is strong evidence for fluorine substitution on the arsenic lattice site.

Our Hall effect data (Fig. 8) were taken on a thinned sample, to minimize the influence of any undoped material further in from the surface than ~10 μm. The data revealed an increase in free electron concentration for the fluorine doped

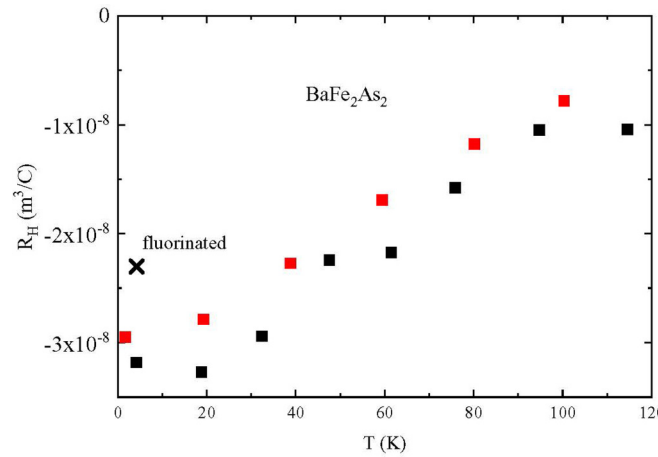

FIG. 8. Hall coefficient measured in 10 T on a thinned, undoped single crystal of $BaFe_2As_2$ (present work, black squares) and data (red squares) on undoped $BaFe_2As_2$ from Fang *et al.* [25]. A data point taken at 4.2 K on the same thinned sample after fluorination (black X) shows, in a simple one band model, an increase in the electron density of 40%.

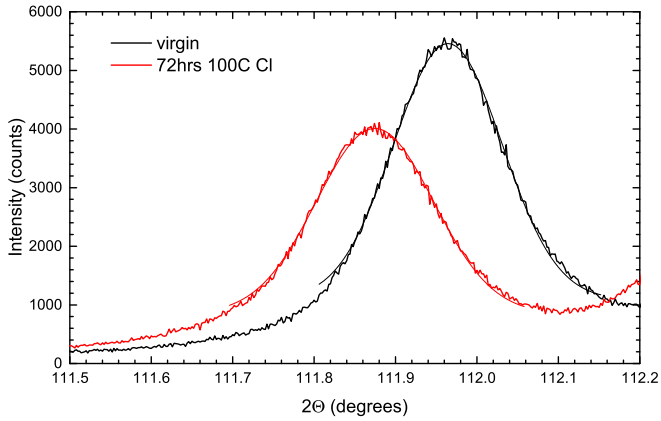

FIG. 9. X-ray diffraction revealing the shift in the (0,0,14) peak between a virgin (black) and chlorinated (red) single crystal.

sample compared to the virgin compound [25,26]. The relatively higher valence of fluorine (−1) to that of arsenic (−3) is analogous to Co-doping for Fe in the 122s. Assuming fully ionized species (a very rough assumption), the role of F can be summarized in the following Kröger-Vink defect reaction equation:

$$F_2 \xrightarrow[BaFe_2As_2]{} 2F_{As}^{\bullet\bullet} + 4e'. \quad (1)$$

Therefore, from the standpoint of a simple one-band model for the Hall effect, we can conclude that the effect of fluorine parallels that of cobalt, donating electrons to the conducting layer and inducing 22 K superconductivity in the nonsuperconducting parent compound.

As has become clear after years of study of the iron-based superconductors, changes in the c-axis parameter are of importance in the discussion of T_c [3,11,27]. Therefore, we were surprised to find that single crystal x-ray diffraction (XRD) on a fluorinated sample showed only minor observable changes in the c-axis lattice parameter. This indicates that the effective atomic radius for F and As in the structure is closer than their direct covalent radius comparison may indicate (Fig. 6). In order to corroborate this, a successive measurement (Fig. 9) on a *chlorinated* single crystal showed a shift in the 2Θ of the (0 0 14) peak of −0.089°, equivalent to an increase in the c axis by 0.027 Å and therefore evidence for an expansion of the lattice. The observed expansion of the lattice is consistent with the substitution of the significantly larger Cl (1.81 Å) atom for As (1.20 Å) (using Shannon's ionic radii [24] as discussed above).

Figure 10 shows EPMA results collected from the surface of an as-grown $BaFe_2As_2$ crystal treated with fluorine. Large surface cracks are observed forming somewhat isolated regions or grains about 15–20 μm in effective diameter. These cracks are the result of the growth process. In terms of composition, it can be seen that both Ba and Fe appear to have higher concentration towards the surface while the As map [Fig. 10(e)] indicates lower composition in the crack regions than in the bulk of the samples. Fluorine [Fig. 10(f)] also shows a similar chemical distribution as As, and more importantly, it is relatively homogenous across the surface. It should

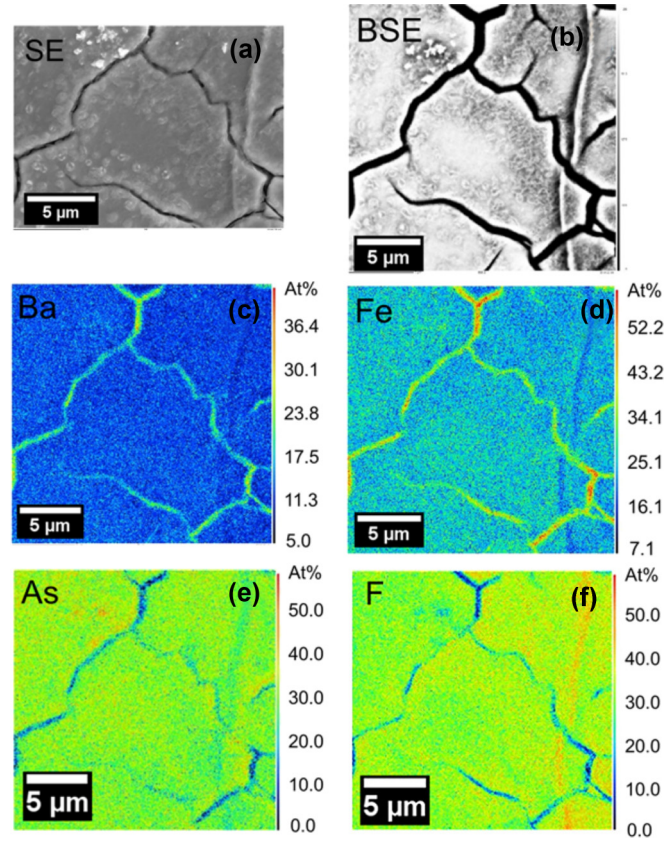

FIG. 10. EPMA elemental mapping analysis of the surface of a $BaFe_2As_2$ crystal treated with fluorine: (a) secondary electron image, (b) backscattered image, (c) Ba, (d) Fe, (e) As, (f) F.

be noted, however, that in some fluorinated samples, we observed islands of noticeably larger fluorine concentration than the surroundings. This inhomogeneity could explain the low critical current density we measure in our samples. Defining the critical current density as the current density required to transition back in the resistivity to the nonsuperconducting state, we obtain a value of 800 A/cm^2. This is an order of magnitude smaller than that reported for the Co electron doped system [18].

In addition, EPMA data (not shown) taken horizontally along a cross-sectional *edge* of the crystal shown in Fig. 2 (rather than the surface as shown in Fig. 10 above) of fluorinated $BaFe_2As_2$ showed that, while the concentrations of Ba and Fe remained relatively constant, the concentrations of As and F were complementary. More importantly, in regions where the concentration of As was small, that of F was large and vice-versa. This is further consistent with the x-ray photoelectron spectroscopy results (a surface measurement) of Fig. 7, and further confirms that F primarily substitutes As.

Moreover, zero-field cooled magnetic susceptibility [28] revealed (Fig. 11) a weak shielding effect at a temperature much lower than that from the resistive transition. These characteristics, namely, low critical current [18,29–31], low critical field [14,29,32], and low T_c could all be consequences of fluorine aggregating into islands [33].

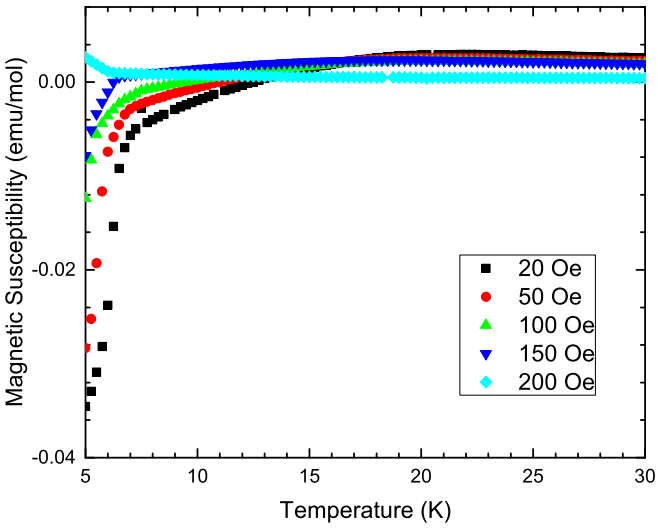

FIG. 11. Field dependence of molar magnetic susceptibility showing a superconducting shielding effect.

C. Discussion of the characterization of the distribution and effect of Cl atoms in $BaFe_2As_2$

In our work to investigate the response of $BaFe_2As_2$ upon exposure to reactive gases to induce superconductivity, we tried several chemicals other than F including I, Br, and Cl, with 3% chlorine in 97% nitrogen gas producing, with certain differences, similar results to those using F. (The effect of Cl on the lattice parameter of $BaFe_2As_2$ was already mentioned above with Fig. 9.) Neither exposure to I nor Br induced superconductivity. One important difference between F and Cl was that chlorination required heating and a significantly longer (days instead of min) treatment time (see Fig. 12) to produce the same effect on the resistance as fluorination. It should be noted, however, that T_c^{onset} remains ~22 K, just like exposure to water vapor [15] and F (current work).

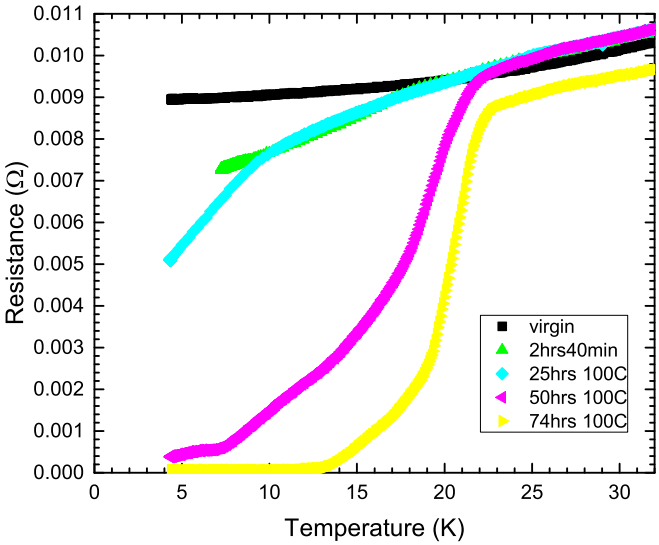

FIG. 12. Timeline of the progression of the temperature dependence of resistance with successive chlorine treatments.

This is an interesting result of the present work; in agreement with exposure to water vapor, apparently reactive gases in general cause the same T_c in 122 $AEFe_2As_2$. Based on the photoemission, EPMA, and Hall effect data on fluorinated samples presented here, this superconductivity is caused by electron doping (F substituting for As) in the FeAs layers of the 122 structure. Although not shown here, it is important to mention that the results of the present work are not restricted to 122 $BaFe_2As_2$ since exposure of $SrFe_2As_2$ to 5% fluorine for 30 min resulted in similar ~22 K superconductivity.

In all cases in the present work of inducing superconductivity, onset T_c measured resistively is always within 2 K of 22 K. This is consistent, as discussed above in the Introduction, with the superconductivity induced in $AEFe_2As_2$ via water vapor [15] and In flux [14]. Though there is a key difference between our work and that [15] of Hiramatsu *et al.* (nanometer thin films vs micron thick reactive layers), it would be interesting if we could find a plausible theory explaining both observed phenomena. Hiramatsu *et al.* conclude that regardless of where the water goes, they have induced superconductivity via chemical pressure but do not rule out the possibility of it being due to a chemical reaction. Chemical pressure, in the current work's case of F doping, is ruled out because of the similarity in size between As and F as supported by our XRD data, at least in the *c*-axis direction.

IV. CONCLUSION

The present work (focused on fluorination of $BaFe_2As_2$, but also with supportive data on chlorination of $BaFe_2As_2$ and fluorination of $SrFe_2As_2$) implies that the long standing puzzle of errant 22 K superconductivity in undoped and water exposed 122 $AEFe_2As_2$ is due to electron doping in the FeAs layers by replacement of As with an electron donor atom. This conclusion is supported by photoemission, EPMA, and Hall effect data.

Also, our work shows that a 20 min exposure to 5% F gas at room temperature is a quick, consistent method to produce superconductivity in 122 iron pnictides. Cl also produces the same superconductivity, but at much longer exposure times (days instead of minutes). The resulting superconducting layer is several μm thick.

ACKNOWLEDGMENTS

The authors would like to acknowledge the advice and cooperation of S. Phillpot, E. Lambers, and D. VanGennep for their help with this research. Work by G.N.T. and G.R.S. supported by the U.S. Department of Energy (DOE), Basic Energy Sciences, Contract No. DE-FG02-86ER45268; work by G.R.S. was also supported by the U.S. DOE Basic Energy Sciences under Contract No. DE-SC-0020385. Work by H.M. and J.C.N. is partially supported by the National Science Foundation under ECCS Award Number 1709641).

Any opinions, findings, and conclusions or recommendations expressed in this material are those of the authors and do not necessarily reflect the views of the National Science Foundation.

[1] Y. Kamihara, H. Hiramatsu, M. Hirano, R. Kawamura, H. Yanagi, T. Kamiya, and H. Hosono, J. Am. Chem. Soc. **128**, 10012 (2006).

[2] Y. Kamihara, T. Watanabe, M. Hirano, and H. Hosono, J. Am. Chem. Soc. **130**, 3296 (2008).

[3] G. R. Stewart, Rev. Mod. Phys. **83**, 1589 (2011).

[4] I. I. Mazin, Nature (London) **464**, 183 (2010).

[5] S. Ishida, D. Song, H. Ogino, A. Iyo, H. Eisaki, M. Nakajima, J.-I. Shimoyama, and M. Eisterer, Phys. Rev. B **95**, 014517 (2017).

[6] P. J. Hirschfeld, M. M. Korshunov, and I. I. Mazin, Rep. Prog. Phys. **74**, 124508 (2011).

[7] A. Chubukov and P. J. Hirschfeld, Phys. Today **68**(6), 46 (2015).

[8] T. Yamazaki, N. Takeshita, R. Kobayashi, H. Fukazawa, Y. Kohori, K. Kihou, C. - H. Lee, H. Kito, A. Iyo, and H. Eisaki, Phys. Rev. B **81**, 224511 (2010).

[9] P. L. Alireza, Y. T. C. Ko, J. Gillett, C. M. Petrone, J. M. Cole, G. G. Lonzarich, and S. E. Sebastian, J. Phys. Condens. Matter **21**, 012208 (2009).

[10] S. A. J. Kimber, A. Kreyssig, Y. - Z. Zhang, H. O. Jeschke, R. Valentí, F. Yokaichiya, E. Colombier, J. Yan, T. C. Hansen, T. Chatterji, R. J. McQueeney, P.C. Canfield, A. I. Goldman, and D. N. Argyriou, Nat. Mater. **8**, 471 (2009).

[11] P. C. Canfield and S. L. Bud'ko, Annu. Rev. Condens. Matter Phys. **1**, 27 (2010).

[12] M. A. Tanatar, N. Ni, G. D. Samolyuk, S. L. Bud'ko, P. C. Canfield, and R. Prozorov, Phys. Rev. B **79**, 134528 (2009).

[13] S. R. Saha, N. P. Butch, K. Kirshenbaum, J. Paglione, and P. Y. Zavalij, Phys. Rev. Lett. **103**, 037005 (2009).

[14] J. S. Kim, T. D. Blasius, E. G. Kim, and G. R. Stewart, J. Phys. Condens. Matter **21**, 342201 (2009).

[15] H. Hiramatsu, T. Katase, T. Kamiya, M. Hirano, and H. Hosono, Phys. Rev. B **80**, 052501 (2009).

[16] S. Nandi, M. G. Kim, A. Kreyssig, R. M. Fernandes, D. K. Pratt, A. Thaler, N. Ni, S. L. Bud'ko, P. C. Canfield, J. Schmalian, R. J. McQueeney, and A. I. Goldman, Phys. Rev. Lett. **104**, 057006 (2010).

[17] X. F. Wang, T. Wu, G. Wu, H. Chen, Y. L. Xie, J. J. Ying, Y. J. Yan, R. H. Liu, and X. H. Chen, Phys. Rev. Lett. **102**, 117005 (2009).

[18] A. S. Sefat, R. Jin, M. A. McGuire, B. C. Sales, D. J. Singh, and D. Mandrus, Phys. Rev. Lett. **101**, 117004 (2008).

[19] X. F. Wang, T. Wu, G. Wu, R. H. Liu, H. Chen, Y. L. Xie, and X. H. Chen, New J. Phys. **11**, 045003 (2009).

[20] M. Nakajima, S. Ishida, T. Tanaka, K. Kihou, Y. Tomioka, T. Saito, C. H. Lee, H. Fukazawa, Y. Kohori, T. Kakeshita, A. Iyo, T. Ito, H. Eisaki, and S. Uchida, Sci. Rep. **4**, 5873 (2014).

[21] G. N. Tam, B. D. Faeth, J. S. Kim, and G. R. Stewart, Phys. Rev. B **88**, 134503 (2013).

[22] M. Nakajima, T. Liang, S. Ishida, Y. Tomioka, K. Kihou, C. H. Lee, A. Iyo, H. Eisaki, T. Kakeshita, T. Ito, and S. Uchida, Proc. Natl. Acad. Sci. U. S. A. **108**, 12238 (2011).

[23] J. S. Kim, G. N. Tam, and G. R. Stewart, Phys. Rev. B **91**, 144512 (2015).

[24] R. D. Shannon, Acta Crystallogr. Sect. A **32**, 751 (1976).

[25] L. Fang, H. Luo, P. Cheng, Z. Wang, Y. Jia, G. Mu, B. Shen, I. I. Mazin, L. Shan, C. Ren, and H.-H. Wen, Phys. Rev. B **80**, 140508(R) (2009).

[26] F. Rullier-Albenque, D. Colson, A. Forget, and H. Alloul, Phys. Rev. Lett. **103**, 057001 (2009).

[27] Y. Han, W. Y. Li, L. X. Cao, X. Y. Wang, B. Xu, B. R. Zhao, Y. Q. Guo, and J. L. Yang, Phys. Rev. Lett. **104**, 017003 (2010).

[28] N. Ni, M. E. Tillman, J. - Q. Yan, A. Kracher, S. T. Hannahs, S. L. Bud'ko, and P. C. Canfield, Phys. Rev. B **78**, 214515 (2008).

[29] Y. Nakajima, T. Taen, and T. Tamegai, J. Phys. Soc. Jpn. **78**, 023702 (2009).

[30] A. Yamamoto, J. Jaroszynski, C. Tarantini, L. Balicas, J. Jiang, A. Gurevich, D. C. Larbalestier, R. Jin, A. S. Sefat, M. A. McGuire, B. C. Sales, D. K. Christen, and D. Mandrus, Appl. Phys. Lett. **94**, 062511 (2009).

[31] R. Prozorov, N. Ni, M. A. Tanatar, V. G. Kogan, R. T. Gordon, C. Martin, E. C. Blomberg, P. Prommapan, J. Q. Yan, S. L. Bud'ko, and P. C. Canfield, Phys. Rev. B **78**, 224506 (2008).

[32] M. Kano, Y. Kohama, D. Graf, F. Balakirev, A. S. Sefat, M. A. Mcguire, B. C. Sales, D. Mandrus, and S. W. Tozer, J. Phys. Soc. Jpn. **78**, 084719 (2009).

[33] C. W. Chu, B. Lv, L. Z. Deng, B. Lorenz, B. Jawdat, M. Gooch, K. Shrestha, K. Zhao, X. Y. Zhu, Y. Y. Xue, and F. Y. Wei, J. Phys. Conf. Ser. **449**, 012014 (2013).